Electronic Supplementary Material (ESI) for Journal of Materials Chemistry A.

Supplementary Information

Fluoride-ion conversion alloy for fluoride-ion batteries

Nakayama et al.

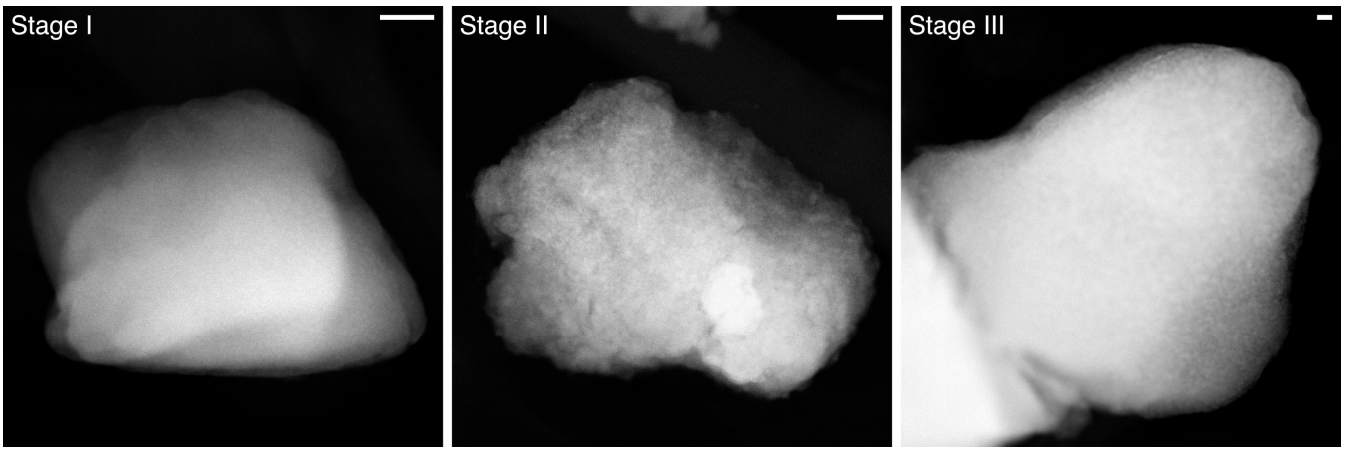

Fig. S1 Low-magnification ADF STEM images of active material particles. The scale bars are 50 nm.

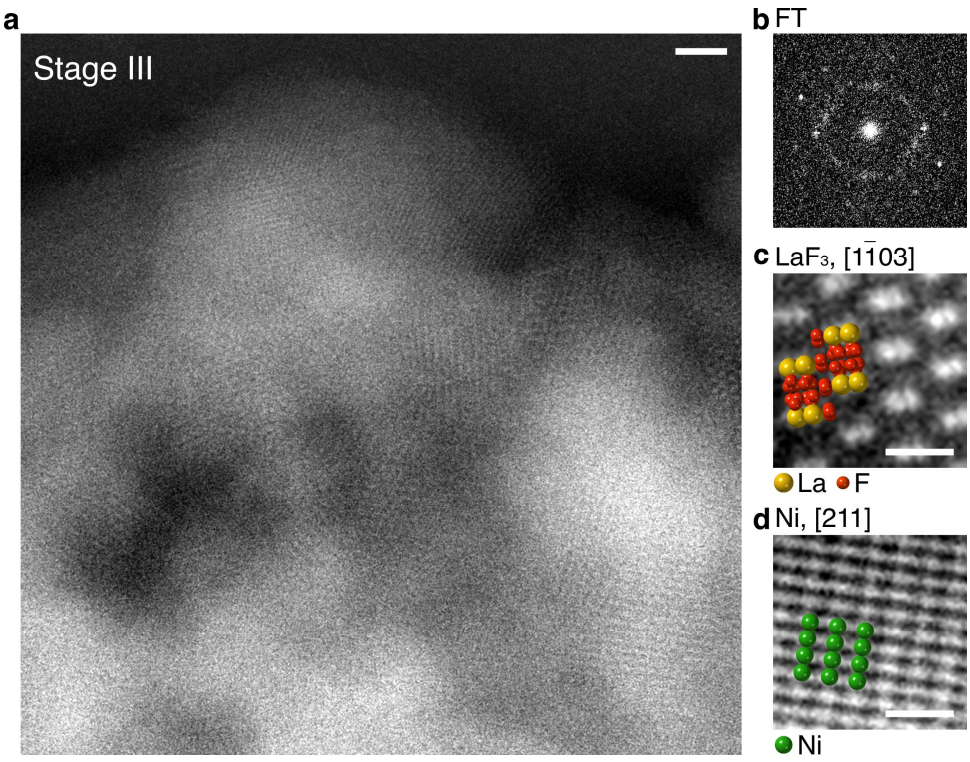

Fig. S2 ADF STEM observation of the sample at the stage-III. (a), (b) ADF STEM image and its Fourier power spectrum obtained from the sample at the stage-III. (c), (d) ADF STEM images of LaF_3 and nickel found in the sample at the stage-III. The scale bar in (a) is 2 nm, and the scale bars in (c), (d) are 0.5 nm.

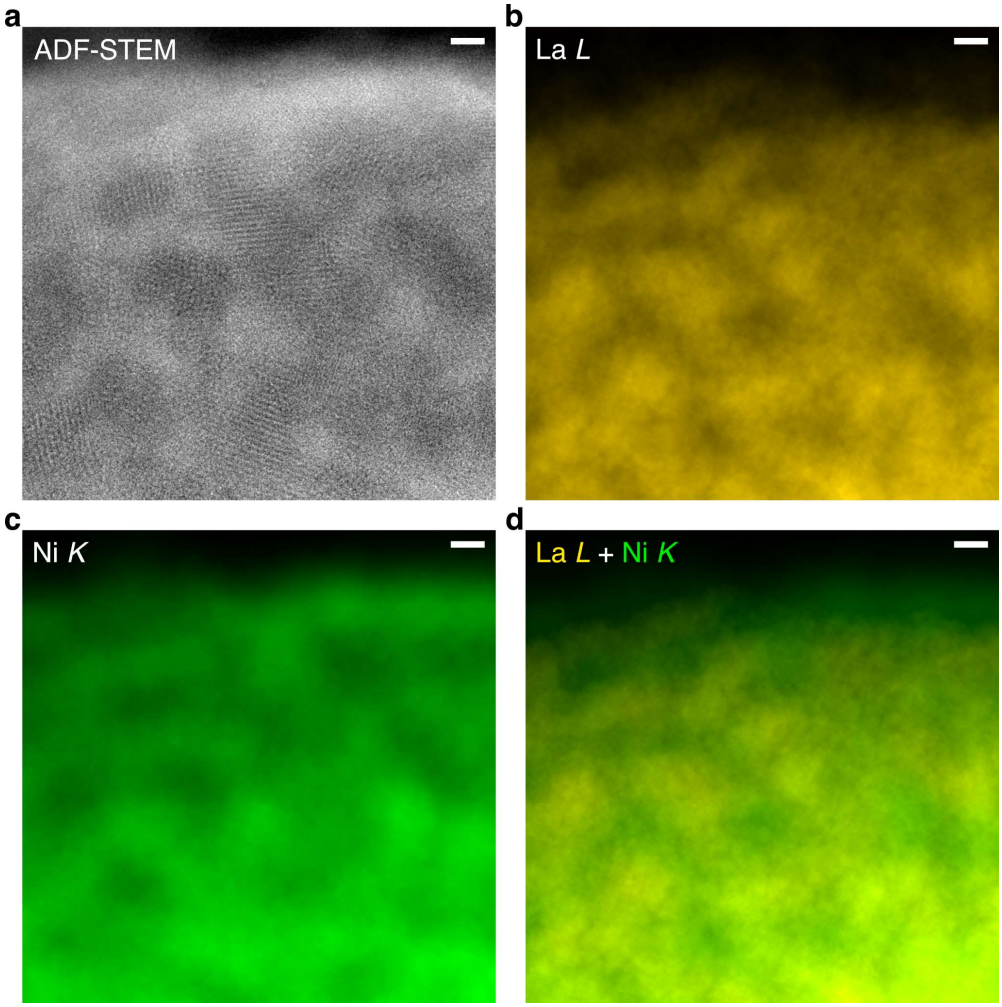

Fig. S3 Shape of nanoscale network formed at the stage-I. (a) ADF STEM image, (b) La-*L* EDX map, and (c) Ni-*K* EDX map obtained from the sample at the stage-I. (d) (La-*L* + Ni-*K*) map obtained by overlaying (b) with (c). The scale bars are 2 nm.

Note S1 As shown in Fig. 1a of the main text, relatively large polarization is found in the stage-II, but only small polarization is observed in the stage-III, which can be interpreted as follows. In the stage-II, the formation of NiF_2 would start from the particle surface as shown in Fig. S4a. At this stage, electrons must flow through LaF_3 or NiF_2, which would increase both the inner resistance and then polarization. On the other hand, at the stage-III, Ni would be formed from the surface as shown in Fig. S4b. Therefore, electric resistivity should be small in Ni, which leads to small polarization.

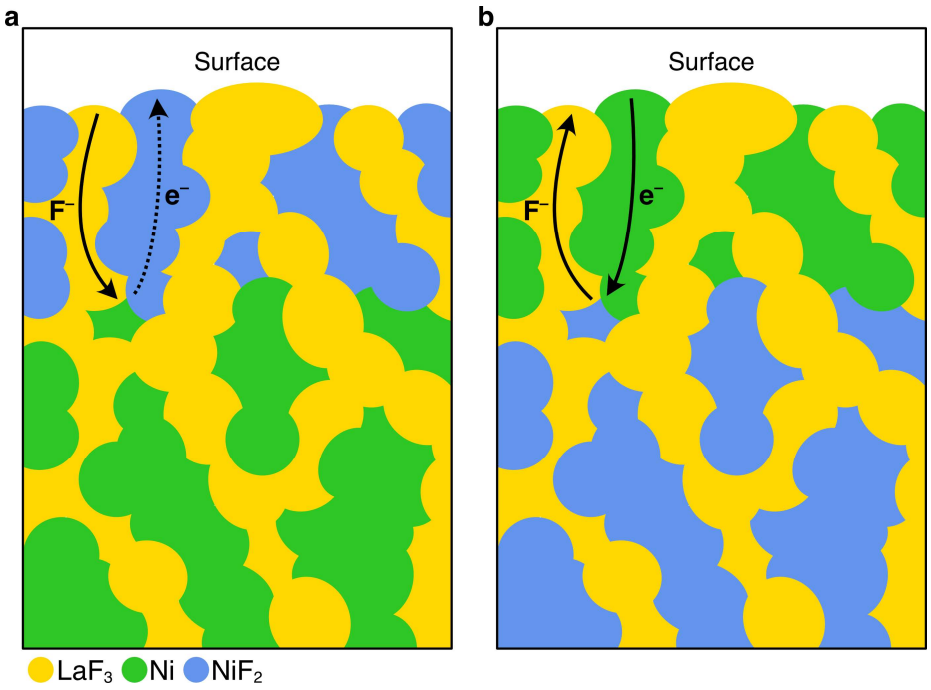

Fig. S4 Schematic views of the nanostructures in the (a) stage-II and (b) stage-III. The yellow, green, and blue regions indicate LaF_3, Ni, and NiF_2, respectively.

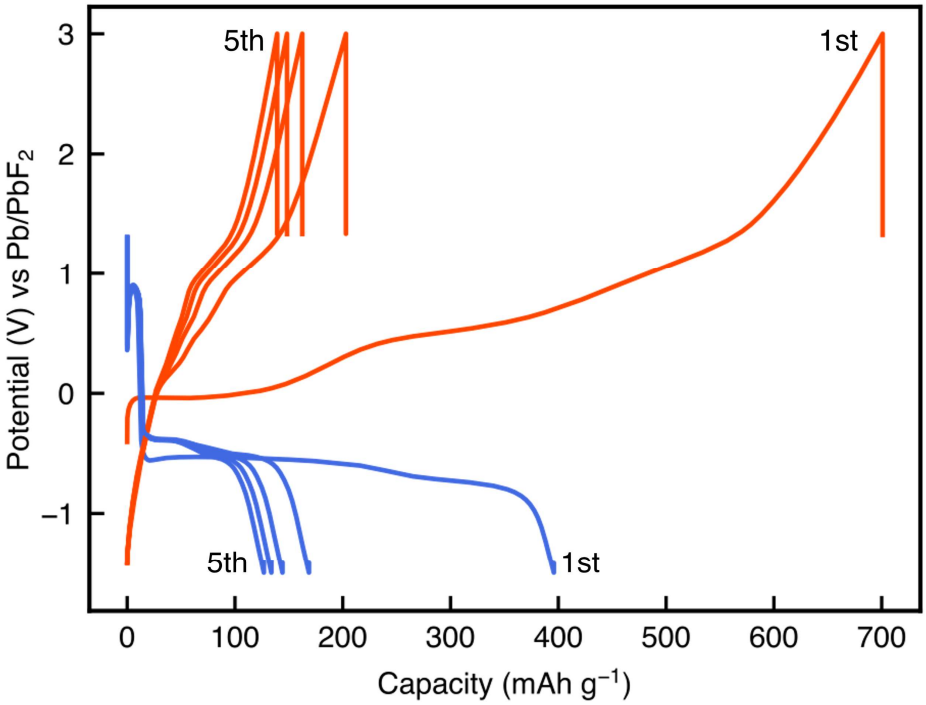

Fig. S5 Charge and discharge curves up to five cycles.

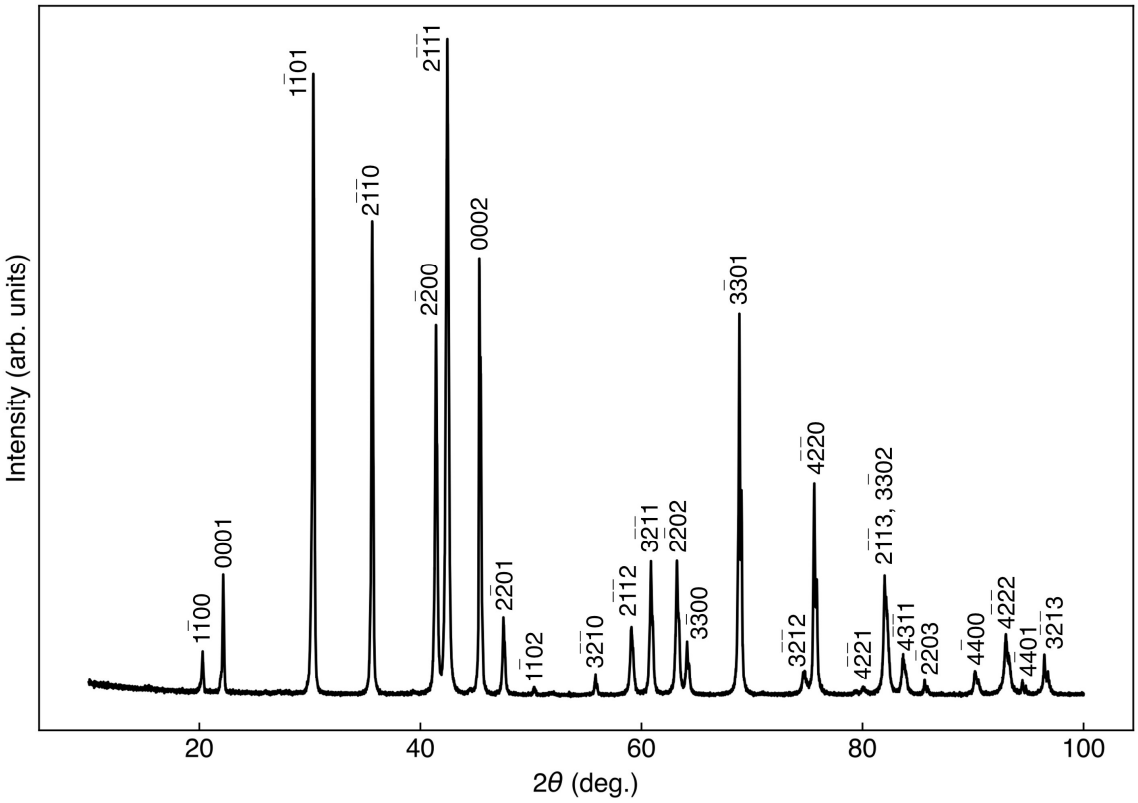

Fig. S6. X-ray powder diffraction profile of pristine $LaNi_5$. All the reflections are indexed based on the hexagonal $LaNi_5$ structure (ref. [1]). This profile was obtained by a SmartLab diffractometer (Rigaku Corp.) using Cu *Kα* radiation.

Note S2 The result of the decomposition of EEL spectra in Fig. 2 is verified by the following two reasons. Firstly, the obtained phase maps are spatially well separated as shown in Fig. 2c, which indicates that the two mathematical components are physically independent. For example, the nanostructure at the stage-III is composed of two phases (LaF_3 and Ni), which is well agreed with ADF images in Fig. S2. It is also noteworthy that the reduction potential of LaF_3 (–2.4 V vs. Pb/PbF_2) is much lower than that in our charge and discharge measurements, and hence LaF_3 should be stable at the stage-III. Secondary, the residual signals are considerably small as shown in Fig. S7, which indicates that the two components should be enough to reproduce the original spectra.

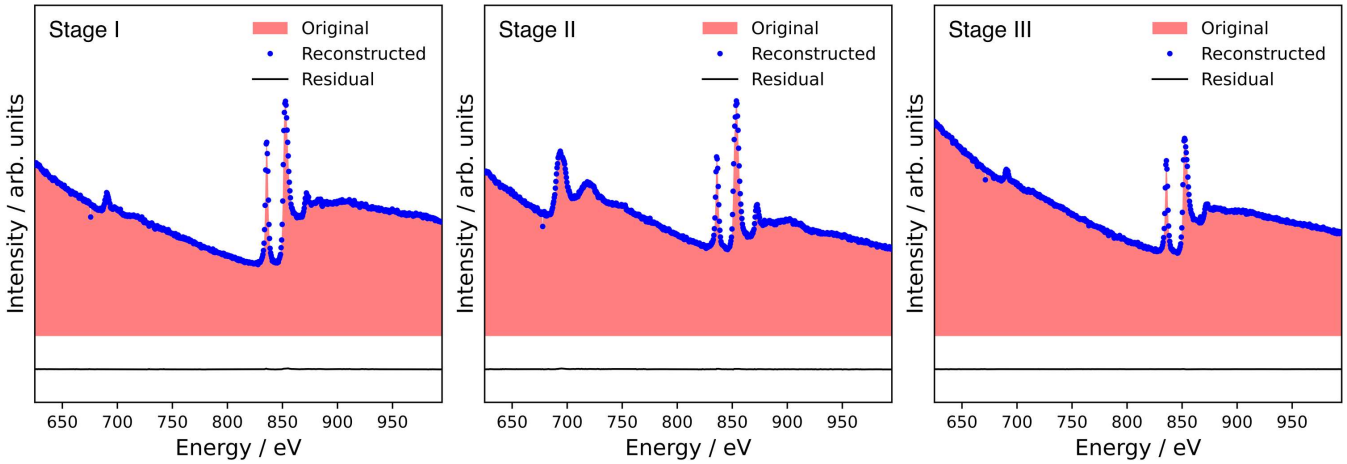

Fig. S7 The residual signals for the decomposed EEL spectra in Fig. 2. The spectra filled with pink show the original spectra, each of which is the sum of the spectra in each region of interest. The blue dots show spectra reconstructed as linear combinations of the decomposed spectra including background signals, and the solid lines show the residual signals.

Reference

[1] J.-M. Joubert, V. Paul-Boncour, F. Cuevas, J. Zhang and M. Latroche, *J. Alloys Compd.*, 2021, **862**, 158163.